International Journal of Multidisciplinary Research and Development
Online ISSN: 2349-4182 Print ISSN: 2349-5979
www.allsubjectjournal.com
Volume 2; Issue 11; November 2015; Page No. 286-292

Hydrodynamic and electro-osmotic transport of aqueous solutions of Pb and Cd nitrate through cellulose acetate membrane

Manoj Kumar, Bali Ram
Department of Chemistry, Centre of Advanced Study, Faculty of Science,
Banaras Hindu University, Varanasi - 221005, U. P., India.

Abstract
Hydrodynamic and electro-osmotic permeability of water and aqueous solutions of $Pb(NO_3)_2$ and $Cd(NO_3)_2.4H_2O$ in the concentration (C) range of 10^{-4} M-10^{-3} M have been measured across cellulose acetate membrane. The data obtained have been used to determine the transport equation using the theory of non-equilibrium thermodynamics. The conductance of membrane-equilibrated with water and aqueous solutions has been measured. Besides, streaming current generated during the transport of various permeants was measured and its dependence on pressure investigated. Phenomenological coefficients have been determined using the transport equation and Saxen's relationship was verified. The zeta potentials have been evaluated using electro-osmotic permeability and membrane-permeant conductance data. It has been observed that hydrodynamic and electro-osmotic permeabilities depend linearly on applied pressure difference and potential difference respectively. Streaming current was also found to depend linearly on applied pressure difference across the membrane.

Keywords: Non-equilibrium thermodynamics, Electro-osmosis, Streaming current and Zeta potential.

1. Introduction

Cellulose acetate (CA) membranes were developed during 1960 [1-2]. CA Membranes are the first type of membranes being used in commercial reverse osmosis (RO) water desalination plants. These membranes are less expensive, have a longer life, require less cleaning, and are much more resistant to chlorine, as compared to other types of RO membranes. CA membrane is a model membrane system, and non-ion selective in nature [3-5] which allows more salt passage and requires higher pressure than other types of membranes. CA membranes have good toughness, high hydrophilicity and relatively low cost, hence they have been widely used for many purposes like, microfiltration, ultrafiltration, reverse osmosis and gas separation [6-7]. CA membranes also have poor chemical resistance, fouling resistance, thermal stability, and mechanical strength [8]. Many surface modification studies have been performed to solve the membrane fouling problem [9].

Membrane technology is a multi-disciplinary separation technique that works without the addition of chemicals and with a relatively low energy use. In chemical technology, membranes have gained an important place and are used in broad range of applications. In some earlier experiments, resistance across the membrane and hydrodynamic flux, J_v, have also been studied [10-13]. According to the theory of non-equilibrium thermodynamics of steady states [14-16] fluxes are coupled, which can be identified using thermodynamic principles. These fluxes obey linear phenomenological relations and a stable steady state. However, it is found that non-equilibrium steady states can also be stable even when the phenomenological relations are nonlinear [17-19].

When a solution passes through a membrane by hydraulic pressure or an electric potential gradient, a series of electro kinetic phenomena occur due to the interaction between the solution and the membrane. Zeta potential gives information about the net charge of the surface and, therefore, about the charge distribution inside the electrical double layer (EDL) [20]. This is due to the surface conductivity of the pores of the membrane and electrical potential. Furthermore, a considerable number of zeta potential conversion theories [21-22] have been elaborated. These theories have taken several aspects and phenomena into account, such as the shape and the size of particles.

This paper presents some interesting results on cellulose acetate membrane which has been obtained during the transport of aqueous solutions of $Pb(NO_3)_2$ and $Cd(NO_3)_2.4H_2O$.The results have been analyzed on the basis of theory of non-equilibrium thermodynamics of irreversible processes. The results obtained with these studies may be helpful in understanding the electrical nature of the membrane-permeant interface [23].

2. Experimental

2.1 Materials

Cellulose acetate membrane (Cat No -190025R) obtained by Axiva Sichem Biotech, New Delhi, was used in the present study. It is hydrophilic in nature having interconnected pores. The membrane was fitted in the permitivity cell for performing the experiment. The salts, $Pb(NO_3)_2$ (Thermo Fisher Scientific, Mumbai) and $Cd(NO_3)_2.4H_2O$ (Qualigens Fine Chemicals, Mumbai) were used as such without further purification to prepare aqueous solutions in doubly distilled water. Aqueous solutions of these salts in the concentration range of 10^{-4} M-10^{-3} M were used as permeants during hydrodynamic permeability, electro-osmotic permeability and streaming current measurements.

2.2 Scanning electron microscopic (SEM) analysis of the membrane

The microstructure of membrane was observed using scanning electron microscope (Model - QUANTA 200 F) before performing the experiment. Images of CA membrane were taken at different magnification range as shown in Figures 1 (a, b and c), for viewing the surface morphology and distribution of pore size in the membrane.

2.3 Measurement of hydrodynamic permeabilities

For the measurements of hydrodynamic permeabilities, an experimental setup, already described by many workers [23-27] was used. The experimental cell was filled with the liquid under investigation, and left as such for 10-12 hours for equilibration before use. For maintaining the equilibrium, the cell was subsequently filled with a degassed fresh solution to confirm that the concentration of the experimental solution remained the same on both sides of the membrane. The volume flux across membrane under various pressure differences was measured by monitoring the movement of liquid-air meniscus in horizontally placed graduated capillary tube with a cross sectional area of 7.86×10^{-3} cm^2. The values of transport coefficients (L_{11}/T) determined from the data on permeability measurement are recorded in the Tables 1-2.

2.4 Measurement of electro-osmotic permeabilities

For measuring of electro-osmotic permeabilities, Pt-electrodes were fitted in the experimental cell in such a way as to touch the membrane from both the sides. Potential differences in the range of 10-50 V were applied across the membrane through these electrodes with the help of an electronically operated power supply (Medox-Bio, Power Supply 300 Advanced). The volumetric flux was measured by following the rate of displacement of the liquid-air meniscus in a horizontally placed graduated capillary tube with a cross sectional area of 7.86×10^{-3} cm^2. The values of electro-osmotic transport coefficients (L_{12}/T) determined from the permeability measurement data are recorded in Tables 1-2. All experiments were carried out in air thermostat maintained at 30 ± 0.5 °C.

2.5 Measurement of Streaming current

Streaming current generated during the transport of permeants by application of various pressure differences on the two sides of the membrane were measured with a Digital Picoammeter (Model PM-100, Raman Scientific Instruments, Roorkee, India) by the technique described elsewhere [25]. The streaming current at lower pressure could not be measured correctly due to less sensitivity of the instruments. The values of electro-osmotic transport coefficients (L_{21}/T) determined from the streaming current measurement data are recorded in Tables 1-2.

2.6 Measurement of membrane conductance

The conductivity of membrane equilibrated with permeants (L_{22}/T) and specific conductance (χ) of permeants were measured with the help of conductivity meter (Systronics-304, cell constant 1 ± 0.1). The values of membrane conductance and specific conductance were found to be in increasing order due to increasing concentrations of the solution and are recorded in the Tables 1-2.

2.7 Determination of viscosity of permeants

Ostwald viscometer was used for determining the viscosity (η) of each solution. The time required for flow of a given volume of solution in between two marks was noted. The following formula [28] has been used for the evaluation of viscosity for all the permeants.

$$\eta_1 = \eta_2 \times \frac{t_1 d_1}{t_2 d_2}$$

Where, η_1 is viscosity of aqueous solutions and η_2 is viscosity of conductivity water.

t_1 is time of flow of aqueous solutions and t_2 is time of flow of conductivity water.

d_1 is density of aqueous solutions and d_2 is density of conductivity water.

An increase in viscosity was obtained with increase in the concentration of solutions due to the resistance in flow. The values of viscosity are recorded in the Tables 1-2.

3. Results and Discussion

Non-equilibrium thermodynamic theory [29] shows that volume flux, J_v, and electrical current, I, under the simultaneous action of pressure difference (ΔP) and electrical potential difference ($\Delta\phi$) are given by:

$$J_v = \frac{L_{11}}{T}(\Delta P) + \frac{L_{12}}{T}(\Delta\phi) \quad (1)$$

$$I = \frac{L_{21}}{T}(\Delta P) + \frac{L_{22}}{T}(\Delta\phi) \quad (2)$$

Where, I is the flow of electricity and the quantities L_{mn} (m, n = 1, 2) are called the phenomenological coefficients.

When, $\Delta\phi = 0$, Eq. (1) reduces to

$$(J_v)_{\Delta\phi=0} = \frac{L_{11}}{T}(\Delta P) \quad (3)$$

Hydrodynamic volume flux, J_v, was found to show a linear dependence on the applied pressure difference, ΔP. The plots of $(J_v)_{\Delta\phi=0}$ against ΔP as shown in Figures 2-3 are straight lines.

When, $\Delta P = 0$, Eq. (1) reduces to

$$(J_v)_{\Delta P=0} = \frac{L_{12}}{T}(\Delta\phi) \quad (4)$$

The electro-osmotic volume flux $(J_v)_{\Delta P=0}$ against $\Delta\phi$ plots are also found linear and shown in Figures 4-5.

The values of phenomenological coefficients (L_{11}/T) and (L_{12}/T), obtained from the slope of linear plots of $(J_v)_{\Delta\phi=0}$ vs. ΔP and $(J_v)_{\Delta P=0}$ vs. $\Delta\phi$ respectively, are recorded in Tables 1-2.

When, $\Delta\phi = 0$; Eq. (2) gives

$$(I)_{\Delta\phi=0} = \frac{L_{21}}{T}(\Delta P) \quad (5)$$

Where $(I)_{\Delta\phi=0}$ is streaming current.

The plots of $(I)_{\Delta\phi=0}$ against ΔP as shown in Figures 6-7 are straight lines, with slopes of giving the values of phenomenological coefficient (L_{21}/T). These values are recorded in Tables1-2.

Following the theory of Overbeek [30] for the flow of liquid through single capillary; we have,

$$\frac{L_{11}}{T} = \frac{\pi r^4}{8\eta\ell} \quad (6)$$

$$\frac{L_{12}}{T} = \frac{\epsilon\, r^2 \xi}{4\eta\ell} \quad (7)$$

$$\frac{L_{22}}{T} = \frac{\pi r^2 \chi}{\ell} \quad (8)$$

If the flow occurs through a membrane which consists of parallel array of *n* capillaries, the right hand side of above equation would increase *n* times. Therefore,

$$\frac{L_{11}}{T} = \frac{n\pi r^4}{8\eta\ell} \quad (9)$$

$$\frac{L_{12}}{T} = \frac{n\epsilon\, r^2 \xi}{4\eta\ell} \quad (10)$$

$$\frac{L_{22}}{T} = \frac{n\pi r^2 \chi}{\ell} \quad (11)$$

An observation of the tables reveals that the values of L_{11}/T decreases with increase in the concentration of permeants which may be attributed to increase in viscosity of permeants. Observation of Tables 1-2, reveals that the values of L_{22}/T i.e. conductance of membrane-equilibrated with permeants are found in increasing order with increase in the concentration of the permeants for all salts. These results are commensurate with the conductance values of the respective solutions. The dependence of L_{22}/T on the concentration of electrolyte solution was found to be in the following sequence $Cd(NO_3)_2.4H_2O > Pb(NO_3)_2 > H_2O$.

Measurement on conductance of membrane-equilibrated with permeants is useful to get insight into the electro-kinetic properties of the membrane porous bodies [31] which depend on the pore size and the zeta potential of the membrane. The electrical conductivity inside the membrane may be higher than the bulk conductivity [32], these effects happen due to high salt concentrations.

In this experiment a non-ion selective CA membrane was used. During electro-osmotic flux measurements, it has been observed that flow of permeants occurred from the positive electrode to the negative electrode. This may happen due to, the electrical potential generated at the membrane-permeant interface as a result of the adsorption of hydrated anions on the membrane surface due to hydrogen bonding with first layer of water on the membrane surface constituting Inner Helmholtz Plane (I.H.P.) and the diffused part of the double layer of the solutions constituting Outer Helmholtz Plane (O.H.P.) [33-34] contains excess of cations as shown in Figure 8. On application of electrical potential gradient, these cations flow from positive electrode to negative electrode i.e. from anode to cathode.

Examination of Tables 1-2 reveals that the values of L_{12}/T (obtained from electro-osmotic transport equation) and L_{21}/T (obtained from streaming current measurement) are nearly equal i.e. $L_{12}/T \approx L_{21}/T$; thereby indicating the validity of Saxen's relationship.

3.1 Morphological studies of CA membrane

The microstructure of the CA membrane was characterized by Scanning Electron Microscopic (SEM) technique. Membrane was snapped in different magnification range (Model - QUANTA 200 F). From the Figures 1 (a, b and c), it becomes clear that at low magnification, the membrane shows very small pore, granule like structure and at high magnification it shows macro pores having different pore sizes as shown in the image. In general, it is thought that morphology of the membrane having granular structure contributes to the sudden increase of solute permeability. Higher porosity of CA membranes was also responsible for the enhanced permeability property. The images were taken with sputtering carbon for producing more electrical conductivity for the determination of morphology of the membranes. To attain high performance of the membrane for specific applications, the morphological structures of the membranes may be manipulated.

3.2 Determination of zeta potential

Generally the zeta potentials of the membranes are supposed to represent the chemical nature of the membrane materials, which is fundamental feature and provides useful information about the electrical charge at solid-liquid surface. Evaluation of zeta potential of membranes is particularly attractive because this quantity is correlated with the mechanism of rejection of charged solutes [35]. In various solutions, electrical nature of the membrane-interfaces can be expressed in terms of zeta potential, which is estimated by combining the electro-osmotic flux coefficient (L_{12}/T) with the membrane-permeants conductance (L_{22}/T).

Zeta potentials from electro-osmotic measurements ($\zeta_{e.o.}$) were estimated from following equation [23, 33-34].

$$\zeta_{e.o.} = \frac{4\pi\eta\chi(L_{12}/T)}{\epsilon(L_{22}/T)} \times 9 \times 10^4\, V \quad (12)$$

Where ϵ is the dielectric constant of the medium used, i.e. water. The values of zeta potentials estimated in this way are recorded in Tables, 1-2. The data for zeta potential obtained from the study on membrane indicate that it increases with increasing concentration for both Lead and Cadmium nitrate solutions which may be attributed to the increase in the thickness of the electrical double layer. The differences in the behavior of zeta potential in all the salts can be explained on the basis of an altered structure of water [36] which is likely to affect the electro-osmotic behavior marginally.

4. Conclusion

Sorption takes place in the membrane matrix due to accumulation of electrolyte ions in membranes. This sorption depends on fixed charge groups and is responsible for the performance of the membrane [37]. Thermodynamic theory of irreversible processes confirms the validity of the linear phenomenological relations, and zeta potential values indicate the existence of electrical charge on membrane surface which also gives the information about the net charge on the surface as well as the charge distribution inside the electric double layer (EDL). The SEM analysis also confirms that CA membrane having different sizes of small pores and fine surface morphology may be useful for numerous purposes in separation areas also. Sometimes evolution of gases occurs at the electrodes due to polarization which may occur when higher electrical potentials are applied across the electrodes; this was, however, minimized by using freshly boiled conductivity water for filling the apparatus.

Table 1: Phenomenological coefficients and Membrane parameters for $Pb(NO_3)_2$ -aqueous systems

C ×10⁴ (M)	$\frac{L_{11}}{T}\times10^{8}$ (cm⁵ sec⁻¹ dyne⁻¹)	$\frac{L_{12}}{T}\times10^{5}$ (cm³ sec⁻¹ V⁻¹)	$\frac{L_{21}}{T}\times10^{5}$ (cm³ sec⁻¹ V⁻¹)	$\frac{L_{22}}{T}\times10^{3}$ (S)	η×10³ (poise)	ϰ ×10³ (S)	ζ e.o. (mV)
0.0	6.59	3.52	3.51	1.40	6.17	3.18	6.970
1.0	6.16	4.12	4.15	1.60	6.24	3.27	7.424
2.0	5.09	4.66	4.28	3.20	6.45	6.60	8.759
4.0	4.72	5.19	5.07	6.20	6.64	12.04	9.456
6.0	4.59	5.67	5.86	9.80	6.84	18.90	10.568
8.0	4.45	6.26	6.18	12.90	7.04	24.80	11.971
10.0	4.42	6.93	6.42	16.80	7.17	31.30	13.080

Table 2: Phenomenological coefficients and Membrane parameters for $Cd(NO_3)_3.4H_2O$-aqueous systems

C ×10⁴ (M)	$\frac{L_{11}}{T}\times10^{8}$ (cm⁵ sec⁻¹ dyne⁻¹)	$\frac{L_{12}}{T}\times10^{5}$ (cm³ sec⁻¹ V⁻¹)	$\frac{L_{21}}{T}\times10^{5}$ (cm³ sec⁻¹ V⁻¹)	$\frac{L_{22}}{T}\times10^{3}$ (S)	η×10³ (poise)	ϰ ×10⁴ (S)	ζ e.o.×10¹ (mV)
0.0	9.27	4.05	3.99	1.80	6.03	4.07	7.802
1.0	6.71	4.49	4.36	2.40	6.07	5.54	8.889
2.0	6.70	4.86	4.82	5.00	6.20	11.24	9.571
4.0	5.87	5.06	5.05	11.50	6.41	24.30	9.684
6.0	5.46	5.29	5.25	16.80	6.55	36.20	10.549
8.0	5.15	5.68	5.57	22.00	6.69	47.70	11.617
10.0	4.73	6.14	6.08	28.00	6.83	60.60	12.825

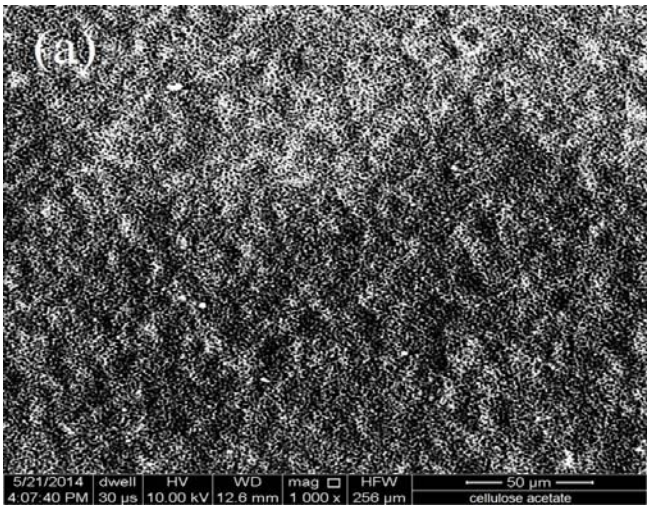

Fig 1: (a) 1,000

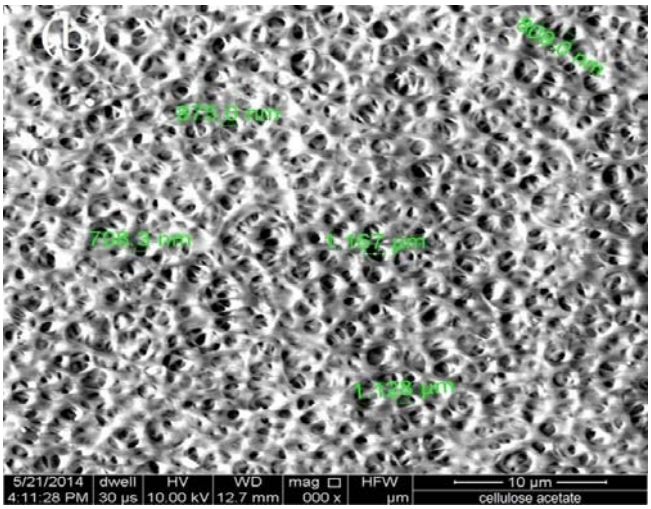

Fig 1: (b) 5,000

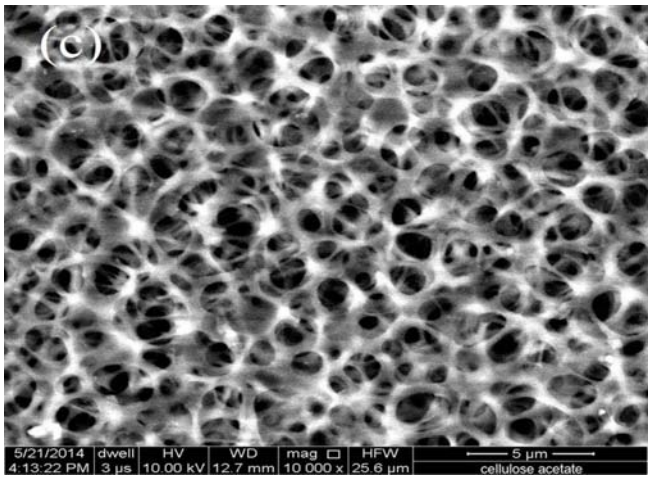

Fig 1: (c) 10,000

Fig 1: SEM images of the top surface area at different magnification:

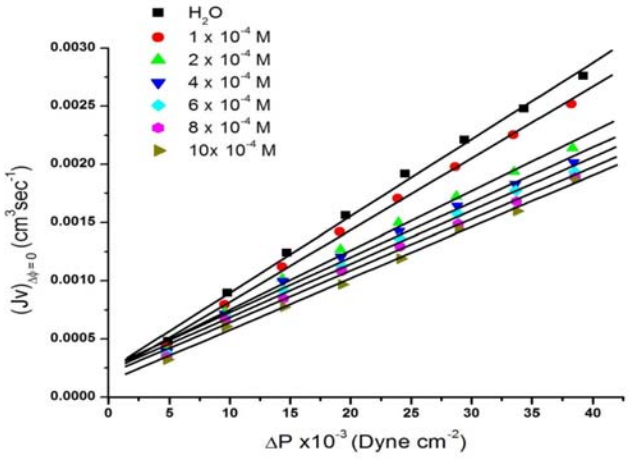

Fig 2: Hydrodynamic permeability for the $Pb(NO_3)_2$-water system

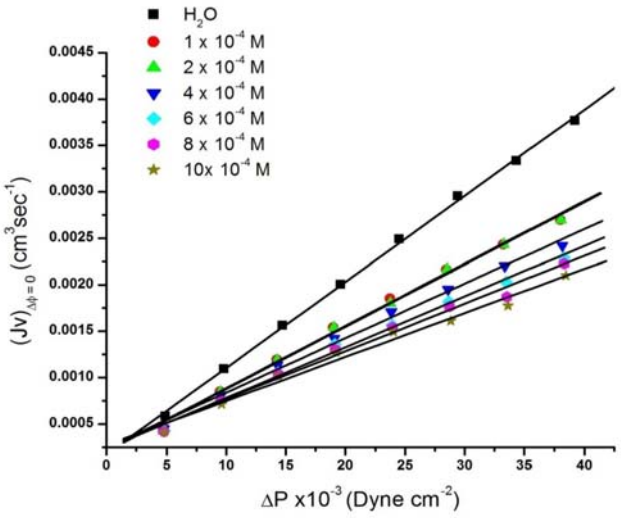

Fig 3: Hydrodynamic permeability for the Cd $(NO_3)_2.4\ H_2O$-water system

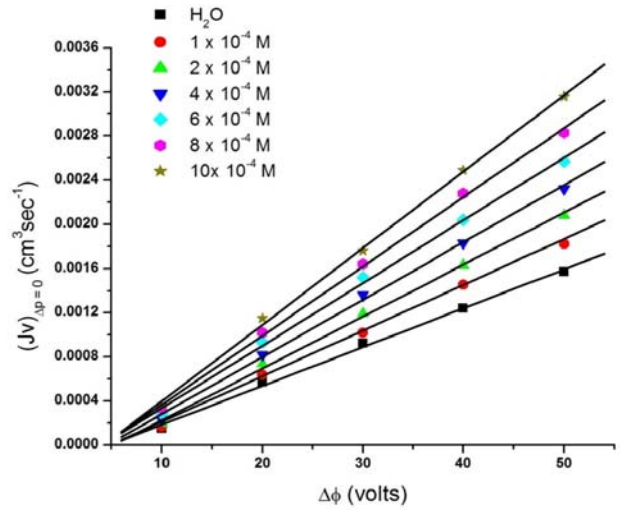

Fig 4: Electro-osmotic flux for Pb $(NO_3)_2$-water system

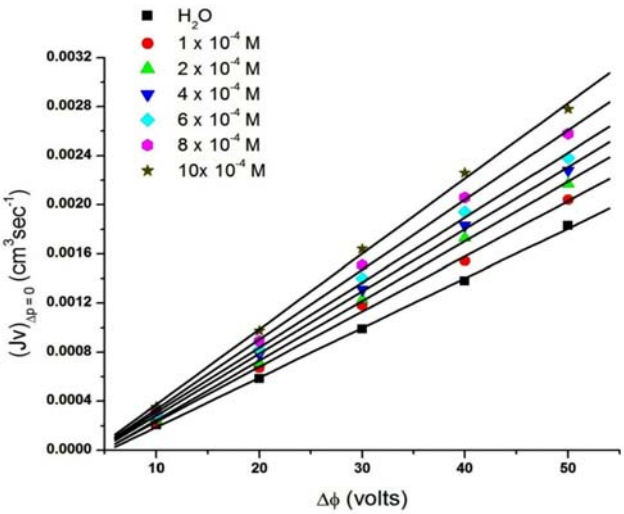

Fig 5: Electro-osmotic flux for Cd $(NO_3)_2.4H_2O$-water system

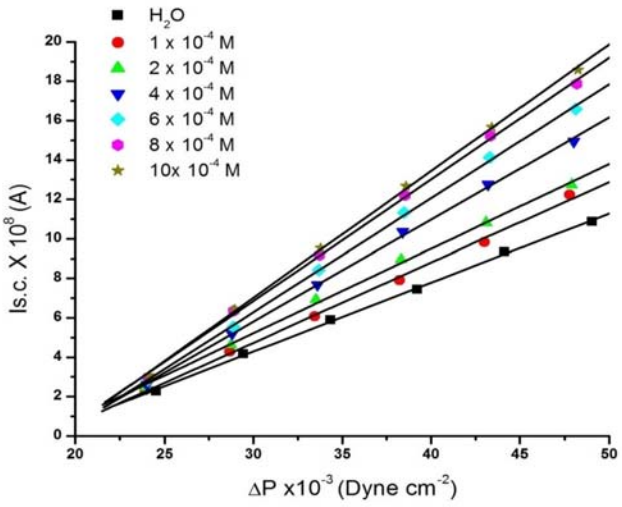

Fig 6: Streaming current for Pb $(NO_3)_2$-water system

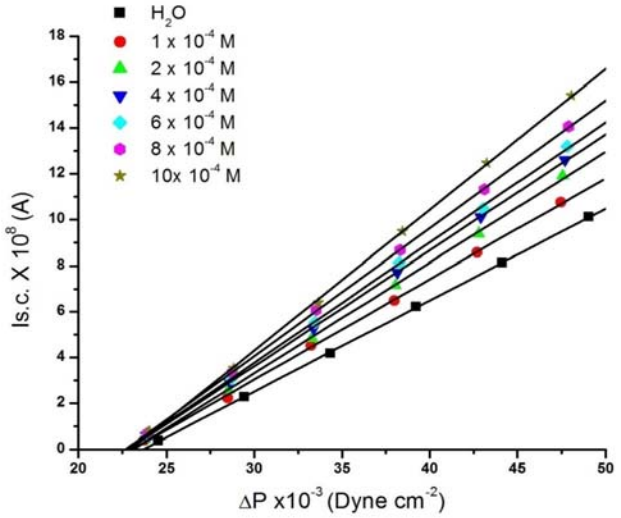

Fig 7: Streaming current flux for Cd $(NO_3)_2.4H_2O$-water system

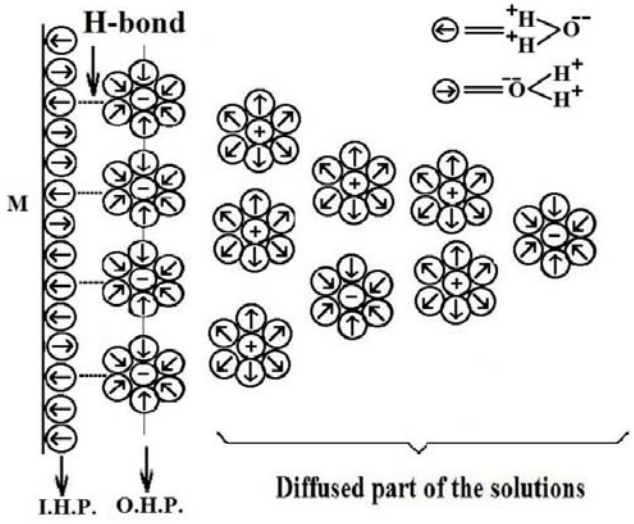

Fig 8: Postulated Picture of the electrical double layer at the Cellulose acetate/aqueous solution interface.

I.H.P. = Inner Helmholtz Plane
O.H.P. = Outer Helmholtz Plane
M = Membrane Surface
$\oplus$ = Cations
$\ominus$ = Anions

Acknowledgments
We would like to thank Banaras Hindu University, Varanasi for laboratory facilities, Department of Metallurgical Engineering, IIT BHU, Varanasi, for SEM analysis and University Grant Commission, New Delhi, for financial support as RGNF.

List of symbols

J_v	Volume flux ($cm^3 sec^{-1}$)
L_{11}	Phenomenological coefficient representing hydrodynamic permeability ($cm^5 sec^{-1} dyne^{-1}$)
L_{12}	Phenomenological coefficient representing electro-osmotic permeability ($cm^3 sec^{-1} V^{-1}$)
L_{21}	Phenomenological coefficient representing streaming potential ($cm^3 sec^{-1} V^{-1}$)
L_{22}	Phenomenological coefficient representing conductivity of the membrane-permeant system (S)
ΔP	Pressure difference (dyne cm^{-2})
I	Electric current (A)
C	Concentration (M)

Greek symbols

ϵ	Dielectric constant of the medium
$\zeta_{e.o.}$	Zeta potential calculated from electro- smotic flux data (mV)
η	Viscosity coefficient (poise)
χ	Specific conductance (S)
$\Delta\phi$	Electrical Potential difference (V)

References

1. Mohammadi T, Saljoughi E. Effect of production conditions on morphology and permeability of asymmetric cellulose acetate membranes, Desalination 2009; 243:1-7.
2. Sivakumar M, Mohan DR, Rangarajan R. Studies on cellulose acetate-polysulfone ultrafiltration membranes II. Effect of additive concentration, J. Membrane Sci. 2006; 268:208-219.
3. Jensen JB, Sorensen TS, Malmgren-Hansen B, Sloth P. Ion-exchange and membrane-potentials in cellulose-acetate membranes separating solutions of mixed electrolytes, J Colloid Interface Sci. 1985; 108:18-30.
4. Singh K, Tiwari AK. Studies on the electrochemical characterization of cellulose acetate and dowex-50 membranes for uni-univalent electrolytes in aqueous solutions, J Colloid Interface Sci. 1999; 210:241-250.
5. Singh K, Tiwari AK, Dwivedi CS. Electrochemical studies on surfactant-modified cellulose acetate membrane, J Colloid Interface Sci. 2003; 266:403-406.
6. Saljoughi E, Sadrzadeh M, Mohammadi T. Effect of preparation variables on morphology and pure water permeation flux through asymmetric cellulose acetate membranes, J Membrane Sci. 2009; 326:627-634.
7. Qin JJ, Li Y, Lee LS, Lee H. Cellulose acetate hollow fiber ultrafiltration membranes madefrom CA/PVP-360K/NMP/water, J Membrane Sci. 218; 2003:173-183.
8. Arthanareeswaran G, Thanikaivelan P. Fabrication of cellulose acetate-zirconia hybrid membranes for ultrafiltration applications: Performance, structure and fouling analysis, Sep. Purif. Technol. 2010; 74:230-235.
9. Ye SH, Watanabe J, Iwasaki Y, Ishihara K. Antifouling blood purification membrane composed of cellulose acetate and phospholipid polymer, Biomaterials 2003; 24:4143-4152.
10. Teorell T. Electrokinetic membrane processes in relation to properties of excitable tissues I. Experiments on oscillatory transport phenomena in artificial membranes, J Gen Physiol. 1959; 42:831-845.
11. Teorell T. Electrokinetic membrane processes in relation to properties of excitable tissues II. Some Theoretical Considerations, J Gen Physiol. 1959; 42:847-863.
12. Meares P, Page KR. Rapid force-flux transitions in highly porous membranes, Philos. Trans. R. Soc. London Ser. A 1972; 272:1-46.
13. Meares P, Page KR. Oscillatory fluxes in highly porous membranes, Proc. R. Soc. London Ser. A 1974; 339:513-532.
14. Prigogine I. Introduction to thermodynamics of irreversible processes, 2nd revised edn. Interscience, New York, 1961.
15. Denbigh KG. Thermodynamics of steady state, Wiley, New York, 1951.
16. De Groot SR. Thermodynamics of irreversible processes, North-Holland, Amsterdam, 1952.
17. Rastogi RP, Srivastava RC, Chand P, Membrane oscillations involving electrokinetic phenomena, J. Colloid Interface Sci. 2003; 263:223-227.
18. Rastogi RP, Srivastava RC, Singh SN, Nonequilibrium thermodynamics of electrokinetic phenomena, Chem. Rev. 1993; 93:1945-1990.
19. Rastogi RP, Srivastava RC, Interface-mediated oscillatory phenomena, Adv. Colloid Interface Sci. 2001; 93:1-75.
20. Bowen WR, Cao XW, Electrokinetic effects in membrane pores and the determination of zeta-potential, J Membrane Sci. 1998; 140:267-273.
21. Szymczyk A, Fievet P, Reggiani JC, Pagetti J. Characterisation of surface properties of ceramic membranes by streaming and membrane potentials, J Membrane Sci. 1998; 146:277-284.
22. Peeters JMM, Mulder MHV, Strathman H. Streaming potential measurements as a characterization method for nanofiltration membranes, Colloids Surf. A: Physicochem. Eng. Aspects 150; 1999:247-259.
23. Srivastava ML, Ram B. Electrokinetic studies of the testosterone- aqueous d-glucose interface, Carbohydr. Res. 1984; 132:209-220.
24. RP. Rastogi, Singh K, Kumar R, Shabd R. Electrokinetic studies on ion-exchange membranes: III. electroosmosis and electrophoresis, J Membrane Sci. 1977; 2:317-331.
25. Srivastava ML, Ram B. Electrokinetic studies on testosterone/aqueous electrolyte interface: Part 1. Electro-osmosis, electrophoresis, streaming potential and streaming current. J Membrane Sci. 1984; 19:137-153.

26. Rastogi RP, Jha KM. Cross-phenomenological coefficients. Part 4.-Electro-osmosis of acetone, Trans. Faraday Soc. 1966; 62:585-594.
27. Kumar M, Ram B. Studies on Nylon-66 membrane using aqueous solutions of potassium and lead nitrate salts as permeants, J Non-Equilib Thermodyn. 2015; 40:13-23.
28. Barnes HA, Hutton JF, Walters K. An Introduction to Rheology, Chapter 2 Elsevier, Amsterdam, 1989.
29. Katchalsky A, Curran PF. Non-equilibrium Thermodynamics in Biophysics, Harvard University Press, Cambridge, MA, 1965.
30. Overbeek JTG, Kruyt HR. Ed., Colloid Science 1, Elsevier, Amsterdam & New York, 1952.
31. Yaroshchuk AE, Luxbacher T. Interpretation of electrokinetic measurements with porous films: role of electric conductance and streaming current within porous structure, Langmuir 2010; 26:10882-10889.
32. Szymczyk A, Fievet P, Aoubiza B, Simon C, Pagetti J. An application of the space charge model to the electrolyte conductivity inside a charged microporous membrane, J Membrane Sci. 1999; 16:1275-285.
33. Shabd R, Upadhyay BM. Electrokinetic studies on carbohydrates, Carbohydr, Res. 1981; 90:187-192.
34. Shabd R, Upadhyay BM. Electrokinetic studies on cholesterol-carbohydrate systems, Carbohydr. Res. 1981; 93:191-196.
35. Labbez C, Fievet P, Thomas F, Szymczyk A, Vidonne A, Foissy A *et al*. Evaluation of the DSPM model on a titania membrane: measurements of charged and uncharged solute retention, electrokinetic charge, pore size, and water permeability, J Colloid Interface Sci. 2003; 262:200-211.
36. Kesting RE. Synthetic Polymeric Membranes, McGraw-Hill, New York, 1971.
37. Tiwari AK, Ahmad S. Studies on electrochemical characterization and performance prediction of cellulose acetate and Zeocarb-225 composite membranes in aqueous NaCl solutions, J Colloid Interface Sci. 2006; 298:274-281.